HHS Public Access

Author manuscript

Chem Commun (Camb). Author manuscript; available in PMC 2016 September 28.

Published in final edited form as:

Chem Commun (Camb). 2015 September 28; 51(75): 14171–14174. doi:10.1039/c5cc04727g.

Functionalized Ultrathin Palladium Nanosheets as Patches for HepG2 Cancer Cells

Yung-Tin Pan[#], **Cartney E. Smith**[#], **Kam Sang Kwok**[#], **Jinrong Chen**, **Hyunjoon Kong**, and **Hong Yang**[*]

University of Illinois at Urbana-Champaign, Department of Chemical and Biomolecular Engineering, 206 Roger Adams Lab, Box C-3, MC-712, 600 South Methews Avenue, Urbana, IL 61801 (USA).

[#] These authors contributed equally to this work.

Abstract

Flexible, charged Pd nanosheets were prepared by using short chain thiolated carboxylic acids and amines. They could wrap around amine or hydroxyl functionalized micron-sized spheres driven by electrostatic interactions. When incubation with HepG2 cells, positively charged cysteamine (CA) functionalized Pd nanosheets exhibited a much higher cytotoxicity, showing more than 80% cell death at 100 ppm than the negatively charged 3-mecaptopropionic acid (MPA) functionalized ones which caused 30% of the cell death. The results show through surface functionalization, Pd nanosheets can be modified to interact differently with HepG2 cancerous cells, resulting in varied cytotoxicity.

Ultrathin two dimensional (2D) nanomaterials such as graphene and palladium are highly flexible and mechanically compatible with soft, biological entities, such as cell and tissue.[1-3] The unique optical properties of these 2D nanomaterials can also be utilized for imaging or photothermal therapy.[4-7] Pd hexagonal sheets with 100 nm edge length and 1-2 nm thickness showed good photothermal stability and were used to kill cancer cells by irradiation of visible light.[8-10] Graphene or graphene oxide nanosheets have been studied for drug delivery.[11-13] However, there are very limited examples on utilizing the geometrical and mechanical properties of ultrathin 2D nanomaterials. To the best of our knowledge, only few studies were carried out using 2D nanosheets: one being graphene oxide (GO) wrapping around *E. coli* bacteria cells and causing them to die due to membrane stress,[14] and another using antibiotic-loaded polysaccharide nanosheets for tissue defect treatment.[15] Such study shows the new opportunity on using 2D nanomaterials for efficient treatment of cancer cells. The intimate contact between the flexible 2D nanosheets and cell surface should enhance the efficiency of drug delivery through on-site release.[16]

[*]Correspondence to: hy66@illinois.edu.

†Electronic Supplementary Information (ESI) available: Materials and methods, Fig. S1-S7, Zeta potential of NH_2-SiO_2 in acetic acid mixed water, Extinction spectra for Pd concentration calibration, concentration calibration curve of Pd nanosheets in water, cell viability of HepG2 cells, SEM of HepG2 cells. See DOI: 10.1039/c000000x/

In this communication, we demonstrate the wrapping of large flexible ultrathin Pd nanosheets around curved substrates, *i.e.*, SiO_2 spheres (500 nm in diameter) through electrostatic interactions. The surface of Pd nanosheets can be made positively or negatively charged by decorating with thiolated carboxylic acid or amine molecules, respectively. Colloidal metal nanostructures can show cytotoxicity, and Au or Ag nanoparticles could be toxic depending on their surface charge.[17-19] Similarly, toxicity of Pd nanosheets towards HepG2 cells was showed to be relevant to the surface charge where positively charged CA-functionalized nanosheets possess significantly higher cytotoxicity than the others. Scanning electron microscope (SEM) study shows the CA-Pd nanosheets were in intimate contact with the HepG2 cells whereas the MPA-Pd nanosheets formed 3D aggregates.

Large 2D Pd nanosheets were synthesized from palladium acetylacetonate ($Pd(acac)_2$) following the procedure reported elsewhere.[20] Briefly, $Pd(acac)_2$ was dissolved in acetic acid, bubbled with carbon monoxide gas for 10 min at room temperature and kept in suspension under closed condition to allow the growth of nanosheets (see Electronic Supplementary Information for experimental and characterization details). The as-made 2D nanosheets were then functionalized with 3-mercaptopropionic acid (MPA) to improve their dispersity in aqueous environment. The colloidal stability originates from the enhanced electrostatic interaction between negatively charged carboxylate group (COO^-) on the surface of Pd nanosheets.

Fig. 1 shows a typical scanning electron microscopy (SEM) image of MPA-stabilized Pd (MPA-Pd) nanosheets. The typical size of MPA-Pd sheets was in the order of microns in terms of lateral dimension and tens of nano meters in thickness. These 2D nanosheets possessed high flexibility due to the high aspect ratio between their lateral dimension and thickness. They were able to wrap closely on the amine-functionalized silica spheres (NH_2-SiO_2, Fig. 2a). The driving force for coating the spheres was likely the electrostatic attraction between the opposite charges on surfaces of MPA-Pd nanosheets and NH_2-SiO_2 spheres.

As a comparison, when negatively charged MPA-Pd nanosheets were mixed with negatively charged HO-SiO_2 spheres, a low degree of coating was observed (Fig. 2b). However, when positively charged CA-functionalized Pd (CA-Pd) nanosheets were mixed with negatively charged HO-SiO_2 spheres, a high degree of coating of nanosheets on the spheres was again observed (Fig. 2c). These observations confirm that the coating of Pd nanosheets on silica spheres was primarily driven by the electrostatic interactions between the charged surface functional groups. A proposed mechanism is presented in Scheme 1. When MPA-Pd nanosheets were mixed with H_2N-SiO_2 spheres in DI water, carboxylic acids on the nanosheet surface deprotonated to form carboxylate anions while amines on the surface of SiO_2 spheres protonated and formed ammonium cations.

Zeta potential measurements were carried out for the two Pd 2D sheets and the two types of silica spheres (Fig. 2d). The Pd nanosheets possessed a potential with negative surface charge of −31.4 ± 2.46 mV for MPA-Pd, and with positive surface charge of 65.7± 2.71 mV for CA-Pd. Similarly, zeta potential of silica spheres was 34.6 ± 2.71 mV for H_2N-SiO_2, and −55.2 ± 4.32 mV for HO-SiO_2. All these surfaces should be highly stable in aqueous

solutions. Moreover, carboxylic acid group on Pd nanosheets should react with NH_2 functional group on SiO_2 spheres in aqueous solution. This interaction further increased the positive potential of NH_2-SiO_2 spheres as compared to the values in Fig. 2d due to the higher extent of amine protonation in acidic environment. As a supporting evidence, self-assembled monolayer (SAM) of MPA has a pK_a value of 5.2~5.6 on gold surface.[21] In our systems, the zeta potential increased to 68 ± 5.33 mV when acetic acid was mixed with NH_2-SiO_2 spheres (Fig. S1). The attraction between the oppositely charged surface carboxylate and ammonium groups drove the formation of stable Pd nanosheets coating onto the SiO_2 spheres. Similar mechanism applies for the coating of CA-Pd nanosheets on HO-SiO_2 spheres. In the latter case, the hydroxyl group deprotonated to O^-, which strongly interacted with NH_3^+ groups coming from the protonation of amine functional group on Pd surface.

The surface-charged Pd nanosheets were incubated with HepG2 cells in order to study their interaction with cell membrane and the dose-dependent cell viability. Fig. 3 shows the fluorescence, bright field, and overlaid images (from left to right) of HepG2 cells incubated with 100 ppm of as-made Pd sheets (Fig. 3a), MPA-Pd nanosheets (Fig. 3b), and CA-Pd nanosheets (Fig. 3c). All the samples were seeded with fluoresceinamine (see supporting information for experimental details on concentration measurements and fluorescent probe labelling, Fig. S2 and Fig. S3).

The fluorescence images show that all three types of Pd nanosheets could attach to HepG2 cells. The bright field image shows Pd nanosheets, the black spots in the images, were on the cells, whose positions were confirmed by the fluorescent images, with different degrees of coverage. The attachment of nanosheets to HepG2 cells had the highest density for the CA-Pd (Fig. 3c), followed by the as-made Pd (Fig. 3a), and the least coverage was observed with the MPA-Pd sample (Fig. 3b), Since HepG2 cells were reported to possess a negatively charged cell surface,[22] positively charged CA-Pd nanosheets possessed higher specificity of cell attachment due to electrostatic attraction compare to the non-charged and negatively charge MPA-Pd nanosheets. In addition to electrostatic forces, the attachment of Pd nanosheets on cell surfaces might also be driven by surface energy minimization and the interaction between the native ligands on cell surface with the Pd nanosheets. This requirement of global energy minimum could attribute to the attachment of MPA-Pd to the cell, albeit with a low coverage, even though these nanosheets were negatively charged.

The cytotoxicity of these Pd nanosheets was examined using the MTT assay (see supporting information for experimental detail). In a typical procedure, HepG2 cells were incubated with Pd nanosheets at the concentrations of 0, 50, and 100 ppm, respectively, for 24 h. Fig. 4 show the dose-dependent cell viability after the exposure to the Pd sheets. Viability results at higher concentrations could not be readily determined accurately because light scatters from the Pd nanosheets causing enough uncertainty in such measurements (Fig. S4).

It was observed that cytotoxicity of Pd nanosheets depends strongly on the types of Pd nanosheets, especially the type of surface functional agent. After 24-h exposure, viability of HepG2 cell was 42.4 ± 11.9% at 50 ppm and 17.93 ± 3.74% at 100 ppm for the CA-Pd nanosheets. In comparison, viability was of 83.7 ± 8.54% at 50 ppm and 68.4 ± 3.9% at 100

ppm for the MPA-Pd nanosheets; and 93.2 ± 6.8% at 50 ppm and 74.7 ± 8.5% at 100 ppm for the as made Pd nanosheets. These data indicate that the difference in cytotoxicity of Pd nanosheets is closely related to the type of surface coating. In the case of MPA-Pd, the nanosheets contacted with HepG2 cells loosely, low and moderate toxicity was observed. The low toxicity was also observed with other negatively charged surfactants, such as polyvinylpyrrolidone (PVP) and polyacrylic acid (PAA), functionalized Pd nanosheets (Fig. S5). On the other hand, CA-Pd nanosheets bound strongly to the surface of HepG2 cells and a high level of cell death at 100 ppm was observed. Control experiments were done using MPA and CA alone with the same protocols for MTT assay. The results show that CA ligands were non-toxic to the HepG2 cells, while MPA at higher concentrations reacted with the MTT reagent, giving rise to artificially high values of cellular viability (Fig. S6). Since CA-Pd and MPA-Pd samples were washed extensively before incubating with HepG2 cells, the concentration of free CA and MPA should be much lower in comparison with those tested in Fig. S6. SEM study on the Pd nanosheets incubated with HepG2 cells were carried out to examine the interaction between the nanosheets and the cell surface. The SEM data suggest that HepG2 cells interacted with Pd nanosheets mainly through electrostatic interaction between the charge Pd nanosheets and the cell surface (Fig. S7). A clear distinction in morphology between the attached MPA-Pd and CA-Pd nanosheets was observed (Fig. S7). In general, MPA-Pd nanosheets tended to crumple to form 3D aggregates instead of lying flat on cell surfaces. Such difference could be due to the repulsive interaction between negative charges on the Pd nanosheets and cell surface. When CA-Pd nanosheets were applied, a significant portion of the cells were in close contact with the nanosheets which tended to stay relatively flat as 2D structures. The high toxicity of positively charged CA-Pd nanosheets is potentially due to the close contact between the sheets and the cell surface which could lead to damage of the cell membrane, agreeing to the previous mentioned work on graphene oxide nanosheets with *E. coli*.[14] In addition, it was reported that graphene nanosheets can cut through the membrane and cause a destructive extraction of large amounts phospholipid from the membrane leading cell death.[23] Thus surface attachment and composition of the nanosheets are important for the observed cytotoxicity.

In summary, large ultrathin Pd nanosheets have been synthesized and further functionalized with CA and MPA ligands in aqueous environments. Due to the flexible nature of 2D nanostructures, the Pd nanosheets are able to wrap around spheres driven by electrostatic interactions between the functionalized nanosheets and surface of spheres. The surface charge of the Pd nanosheets greatly affects the physical contact nature and its toxicity to HepG2 cells. Positively charged CA-Pd nanosheets possessed high-level contact with the cell membrane as 2D patches while negatively charged MPA-Pd nanosheets formed aggregates. The CA-Pd nanosheets were three times more toxic than the MPA-Pd nanosheets at 100 ppm based on MTT assay, indicating the important effect of surface ligands of these 2D nanosheets on cytotoxicity. This study demonstrates the potential of using ultrathin metal nanosheets as carriers for drug delivery and targeted release through surface modification with ligands that contain specific, therapeutic functional groups.

Supplementary Material

Refer to Web version on PubMed Central for supplementary material.

Acknowledgments

This work is supported in part by University of Illinois Start-up Fund, National Science Foundation (STC-EBICS Grant, CBET-0939511), and the National Institute of Health (1R01 HL109192). SEM and zetapotential measurements were carried out at the Frederick Seitz Materials Research Laboratory Central Research Facilities, UIUC. Fluorescent imaging was carried out in the Imaging Technology Group, Beckman Institute at UIUC. We thank Lou Ann Millier for the preparation of biological SEM specimen. Y.T.P. is grateful for fellowships from Ministry of Education of Taiwan and Dow Chemical Company.

Notes and references

1. Hwang S-W, Tao H, Kim D-H, Cheng H, Song J-K, Rill E, Brenckle MA, Panilaitis B, Won SM, Kim Y-S, Song YM, Yu KJ, Ameen A, Li R, Su Y, Yang M, Kaplan DL, Zakin MR, Slepian MJ, Huang Y, Omenetto FG, Rogers JA. Science. 2012; 337:1640–1644. [PubMed: 23019646]
2. Kim KS, Zhao Y, Jang H, Lee SY, Kim JM, Kim KS, Ahn J-H, Kim P, Choi J-Y, Hong BH. Nature. 2009; 457:706–710. [PubMed: 19145232]
3. Eda G, Fanchini G, Chhowalla M. Nat. Nanotechnol. 2008; 3:270–274. [PubMed: 18654522]
4. Yin W, Yan L, Yu J, Tian G, Zhou L, Zheng X, Zhang X, Yong Y, Li J, Gu Z, Zhao Y. ACS Nano. 2014; 8:6922–6933. [PubMed: 24905027]
5. Liu T, Wang C, Gu X, Gong H, Cheng L, Shi X, Feng L, Sun B, Liu Z. Adv. Mater. 2014; 26:3433–3440. [PubMed: 24677423]
6. Hu W, Peng C, Luo W, Lv M, Li X, Li D, Huang Q, Fan C. ACS Nano. 2010; 4:4317–4323. [PubMed: 20593851]
7. Cheng L, Liu J, Gu X, Gong H, Shi X, Liu T, Wang C, Wang X, Liu G, Xing H, Bu W, Sun B, Liu Z. Adv. Mater. 2014; 26:1886–1893. [PubMed: 24375758]
8. Huang X, Tang S, Mu X, Dai Y, Chen G, Zhou Z, Ruan F, Yang Z, Zheng N. Nat. Nanotechnol. 2011; 6:28–32. [PubMed: 21131956]
9. Fang W, Tang S, Liu P, Fang X, Gong J, Zheng N. Small. 2012; 8:3816–3822. [PubMed: 22903778]
10. Tang S, Chen M, Zheng N. Nano Res. 2015; 8:165–174.
11. Liu K, Zhang J-J, Cheng F-F, Zheng T-T, Wang C, Zhu J-J. J. Mater. Chem. 2011; 21:12034–12040.
12. Rana VK, Choi M-C, Kong J-Y, Kim GY, Kim MJ, Kim S-H, Mishra S, Singh RP, Ha C-S. Macromol. Mater. Eng. 2011; 296:131–140.
13. Pandey H, Parashar V, Parashar R, Prakash R, Ramteke PW, Pandey AC. Nanoscale. 2011; 3:4104–4108. [PubMed: 21909583]
14. Liu S, Zeng TH, Hofmann M, Burcombe E, Wei J, Jiang R, Kong J, Chen Y. ACS Nano. 2011; 5:6971–6980. [PubMed: 21851105]
15. Toshinori Fujie AS, Kinoshita Manabu, Miyazaki Hiromi, Ohtsubo Shinya, Saitoh Daizoh, Takeoka Shinji. Biomaterials. 2010; 31:6269–6278. [PubMed: 20493525]
16. Cheng H, Kastrup CJ, Ramanathan R, Siegwart DJ, Ma M, Bogatyrev SR, Xu Q, Whitehead KA, Langer R, Anderson DG. ACS Nano. 2010; 4:625–631. [PubMed: 20121215]
17. Goodman CM, McCusker CD, Yilmaz T, Rotello VM. Bioconjugate Chem. 2004; 15:897–900.
18. El Badawy AM, Silva RG, Morris B, Scheckel KG, Suidan MT, Tolaymat TM. Environ. Sci. Technol. 2011; 45:283–287. [PubMed: 21133412]
19. Boisselier E, Astruc D. Chem. Soc. Rev. 2009; 38:1759–1782. [PubMed: 19587967]
20. Yin X, Liu X, Pan Y-T, Walsh KA, Yang H. Nano Lett. 2014
21. Zhao J, Luo L, Yang X, Wang E, Dong S. Eelctroanal. 1999; 11:1108–1113.
22. Saravia V, Toca-Herrera JL. Microsc. Res. Techniq. 2009; 72:957–964.

23. Tu Y, Lv M, Xiu P, Huynh T, Zhang M, Castelli M, Liu Z, Huang Q, Fan C, Fang H, Zhou R. Nat. Nanotechnol. 2013; 8:594–601. [PubMed: 23832191]

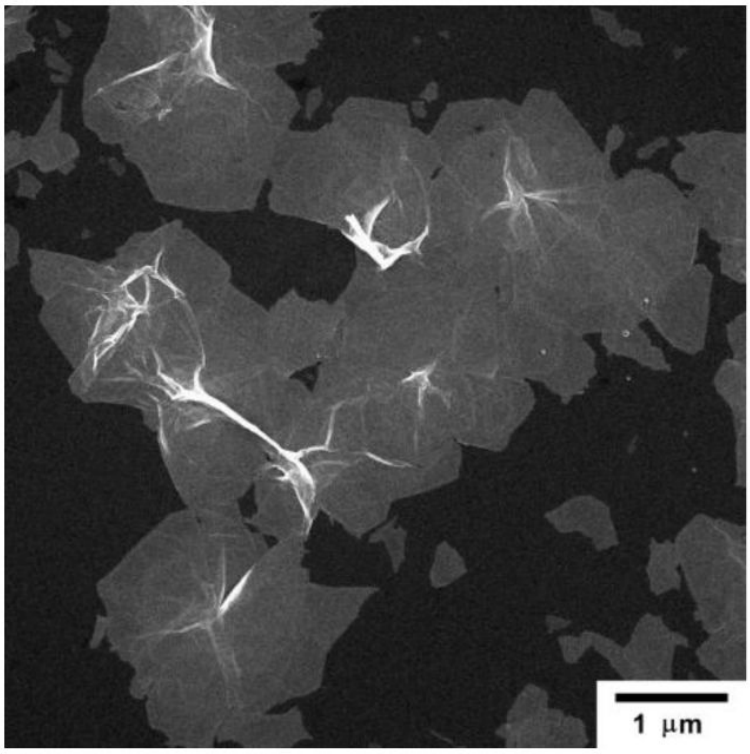

Fig. 1.
SEM micrograph of MPA-Pd nanosheets deposited on Al foil.

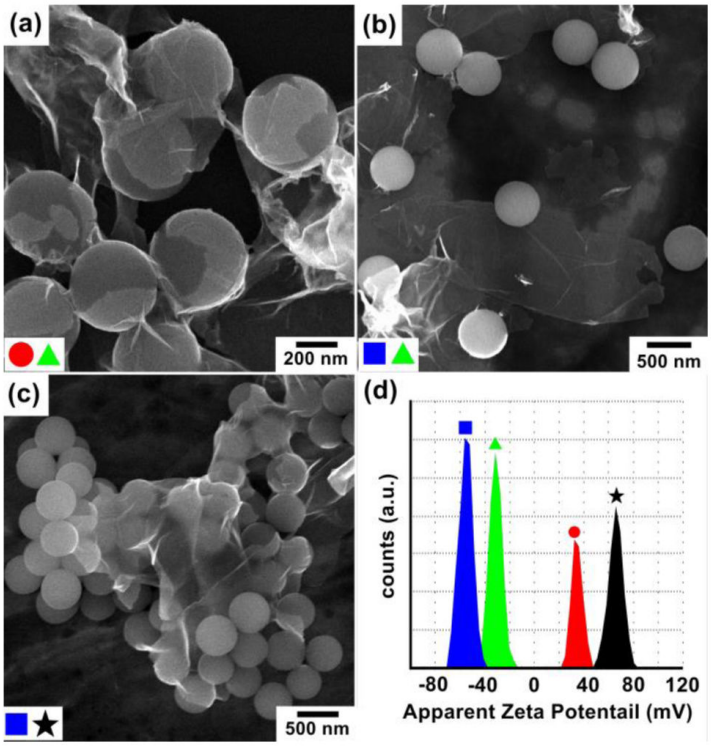

Fig. 2.

SEM micrographs of Pd nanosheets mixed with silica spheres: (a) MPA-Pd with NH_2-SiO_2, (b) MPA-Pd with HO-SiO_2, (c) H_2N-Pd with HO-SiO_2, and (d) zeta potential measurement of functionalized Pd nanosheets and silica spheres: (▪) HO-SiO_2; (▲) MPA-Pd; (●) H_2N-SiO_2; and (★) H_2N-Pd.

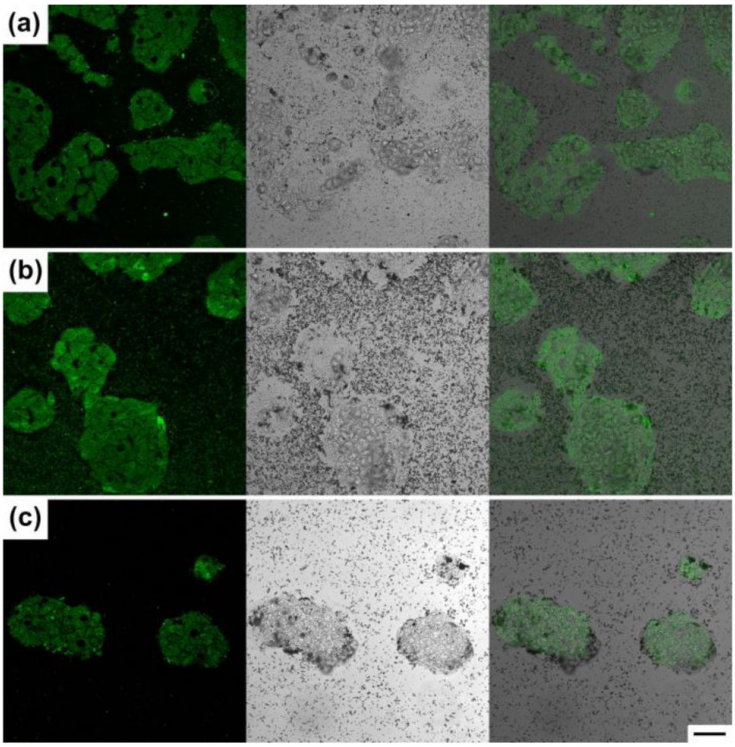

Fig. 3.

Fluorescence, bright field microscope images and overlays of HepG2 cells incubated with 100 ppm of (a) as-made Pd; (b) MPA-Pd; and (c) CA-Pd nanosheets. All specimen were labelled with fluoresceinamine. Scale bar is 50 μm, applicable to all images.

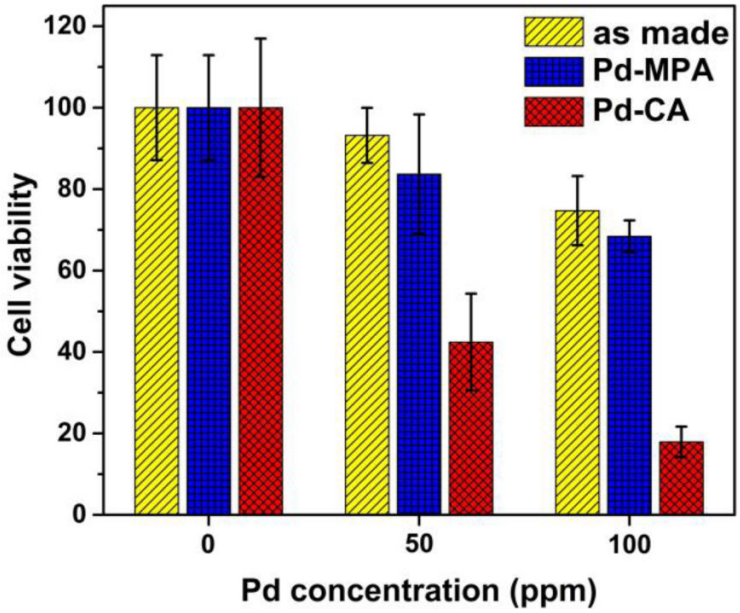

Fig. 4.

Viability study of HepG2 cells incubated with as-made, MPA functionalized, and CA functionalized Pd sheets by MTT assay.

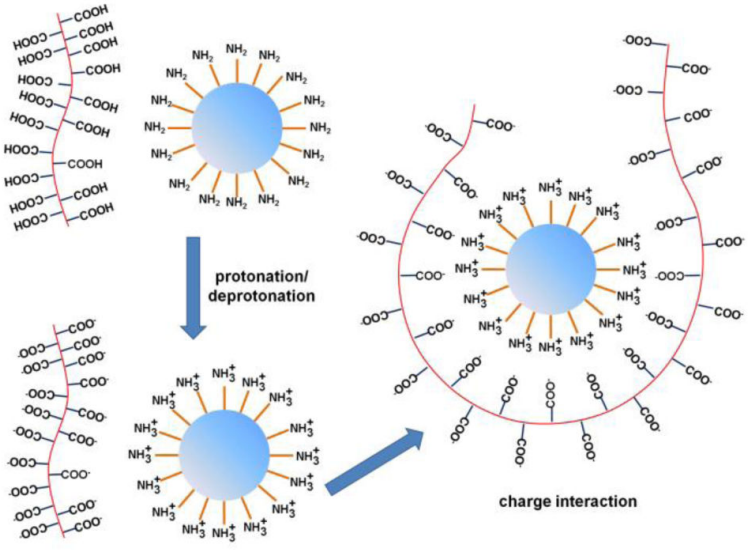

Scheme 1.
Illustration of MPA-Pd nanosheets wrapping around NH_2-SiO_2 spheres.